

Optimization of 3-Pyrimidin-4-yl-oxazolidin-2-ones as Allosteric and Mutant Specific Inhibitors of IDH1

Julian Roy Levell, Thomas Caferro, Gregg Chenail, Ina Dix, Julia Dooley, Brant Firestone, Pascal D Fortin, John Giraldes, Ty Gould, Joseph D. Growney, Michael D Jones, Raviraj Kulathila, Fallon Lin, Gang Liu, Arne Mueller, Simon van der Plas, Kelly Slocum, Troy Smith, Remi Terranova, B. Barry Touré, Viraj Tyagi, Trixie Wagner, Xiaoling Xie, Ming Xu, Fan Yang, Liping X. Zhou, Raymond Pagliarini, and Young Shin Cho

ACS Med. Chem. Lett., **Just Accepted Manuscript** • DOI: 10.1021/acsmedchemlett.6b00334 • Publication Date (Web): 16 Dec 2016

Downloaded from <http://pubs.acs.org> on December 19, 2016

Just Accepted

“Just Accepted” manuscripts have been peer-reviewed and accepted for publication. They are posted online prior to technical editing, formatting for publication and author proofing. The American Chemical Society provides “Just Accepted” as a free service to the research community to expedite the dissemination of scientific material as soon as possible after acceptance. “Just Accepted” manuscripts appear in full in PDF format accompanied by an HTML abstract. “Just Accepted” manuscripts have been fully peer reviewed, but should not be considered the official version of record. They are accessible to all readers and citable by the Digital Object Identifier (DOI®). “Just Accepted” is an optional service offered to authors. Therefore, the “Just Accepted” Web site may not include all articles that will be published in the journal. After a manuscript is technically edited and formatted, it will be removed from the “Just Accepted” Web site and published as an ASAP article. Note that technical editing may introduce minor changes to the manuscript text and/or graphics which could affect content, and all legal disclaimers and ethical guidelines that apply to the journal pertain. ACS cannot be held responsible for errors or consequences arising from the use of information contained in these “Just Accepted” manuscripts.

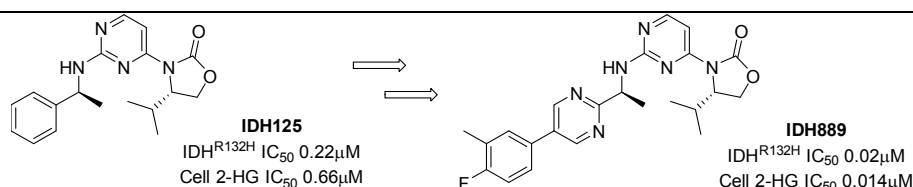


Optimization of 3-Pyrimidin-4-yl-oxazolidin-2-ones as Allosteric and Mutant Specific Inhibitors of IDH1

Julian R. Levell, Thomas Caferro, Gregg Chenail, Ina Dix, Julia Dooley, Brant Firestone, Pascal D. Fortin, John Giraldez, Ty Gould, Joseph D. Growney, Michael D. Jones, Raviraj Kulathila, Fallon Lin, Gang Liu, Arne Mueller, Simon van der Plas, Kelly Slocum, Troy Smith, Remi Terranova, B. Barry Touré, Viraj Tyagi, Trixie Wagner, Xiaoling Xie, Ming Xu, Fan S. Yang, Liping X. Zhou, Raymond Pagliarini,* and Young Shin Cho*

Novartis Institutes for Biomedical Research, 250 Massachusetts Avenue, Cambridge, MA 02139

KEYWORDS mutant IDH1 inhibitor, allosteric inhibition, 2-HG, preclinical in-vivo activity, 3-pyrimidin-4-yloxazolidin-2-one, chirality-defined potency



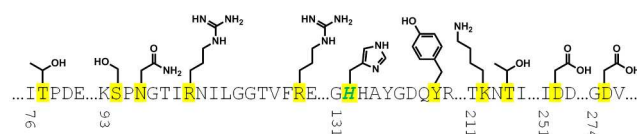
ABSTRACT: High throughput screening and subsequent hit validation identified 4-isopropyl-3-(2-((1-phenylethyl)amino)pyrimidin-4-yl)oxazolidin-2-one as a potent inhibitor of IDH1^{R132H}. Synthesis of the four separate stereoisomers identified the (S,S)-diastereomer (**IDH125**, **1f**) as the most potent isomer. This also showed reasonable cellular activity and excellent selectivity vs. IDH1^{wt}. Initial SAR exploration identified the key tolerances and potential for optimization. X-ray crystallography identified a functionally relevant allosteric binding site amenable to inhibitors which can penetrate the blood-brain barrier, and aided rational optimization. Potency improvement and modulation of the physico-chemical properties identified (S,S)-oxazolidinone **IDH889** (**5x**) with good exposure and 2-HG inhibitory activity in a mutant IDH1 xenograft mouse model.

Hotspot heterozygous mutations in human cytoplasmic isocitrate dehydrogenase 1 (IDH1) at Arg¹³² (R132*) have been identified in multiple cancer types, including acute myeloid leukemia (AML), glioma, chondrosarcoma and cholangiocarcinoma.¹ These mutations have been shown to confer a neomorphic catalytic activity to produce high levels of intracellular R-2-hydroxyglutarate (2-HG) and effect downstream epigenetic markers on DNA and proteins.^{2,3} Catalytic inhibitors⁴⁻¹⁰ of IDH1^{R132*} have shown preclinical reduction of 2-HG levels in xenograft mouse models with mutant IDH1 tumors, and have also shown preclinical tumor regression.⁴⁻⁷ Recent clinical trials in AML patients with a specific inhibitor of IDH1 has shown clinical benefit, confirming the causal link between this genetic mutation, the production of 2-HG, and cancer.¹¹ Efforts herein focused on the identification of compounds which could potentially target all classes of mutant-IDH1 tumors, including those in the brain.

The substrate-binding site of mutant IDH1 is highly polar as defined by the amino acids lining the pocket (Figure 1), in addition to the active-site magnesium ion and NADPH cofactor. This suggests a low probability of being able to optimize a compound for potent binding to this site whilst also fulfilling the criteria most conducive to crossing the blood-brain barrier (BBB).¹² It was decided to explore the identification of catalytic

inhibitors with different mechanisms of action, which may bind distal to this polar substrate-binding site.

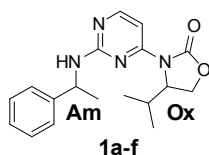
Figure 1: Sequence and sidechain representation of the substrate-binding site for IDH1^{R132H}. Amino acids lining the pocket are highlighted in yellow, mutation site R132H is shown in green.



High throughput screening was carried out with a NADPH fluorescence-based biochemical assay using IDH1^{R132H} homodimer protein, and orthogonal biochemical inhibition confirmation using an LCMS readout of 2-HG levels. Compounds **1a** and **1b** were identified as selective and functional inhibitors of IDH1^{R132H} from this screen. Both **1a** and **1b** were screened as diastereomeric mixtures at the amine (Table 1, Am), which necessitated the independent synthesis of the four separate stereoisomers in order to determine the chiral preference for ligand binding. Potency was found to be most strongly dependent upon the chirality at the amine center (Am), although still significantly affected by the chirality at the oxazolidinone (Ox) (Table 1). The preference for the S-amine isomer was maintained throughout the SAR on the series, but the ef-

fect of *R*-chirality at the oxazolidinone was sometimes only marginal. As described elsewhere,¹³ compound **1f** (**IDH125**) was validated with multiple biophysical methods and this compound enabled considerable understanding of the rationale for selectivity and mechanism of action of this series. **IDH125** was also confirmed as an essentially equipotent inhibitor of both the homodimer IDH1^{R132H} (IC₅₀ 0.22 μM) and IDH1^{R132C} (IC₅₀ 0.15 μM) proteins and slightly less potent for the heterodimer IDH1^{wt}-IDH1^{R132H} (IC₅₀ 0.97 μM) protein using NADPH fluorescence-based biochemical assay.¹³ The cancer-specific mutation of IDH1 and lack of activity of **IDH125** against wild-type IDH1 up to 50 μM presented an opportunity to develop an oncology drug with a high therapeutic index.

Table 1. IDH1^{R132H} biochemical activity of HTS hits and pure resynthesized diastereomers.

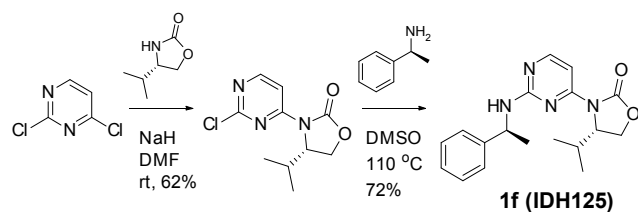


	Chirality at amine (Am)	Chirality at oxazolidinone (Ox)	Biochem. LCMS IC ₅₀ / μM
1a	R:S = 1:1	S	0.8
1b	R:S = 1:1	R	8.5
1c	R	R	19.7
1d	S	R	4.2
1e	R	S	4.6
1f (IDH125)	S	S	0.22

It was noted that **IDH125** contains an aminopyrimidine core, which is a common motif in ATP-competitive kinase inhibitor scaffolds due to the structural similarity vs. the purine nucleus of ATP.¹⁴ Therefore, initial thorough kinase profiling of **IDH125** in an internal kinase profiling panel, as well as an external kinase profiling panel was carried out (supporting information) **IDH125** demonstrated virtually no inhibitory activity across the entire kinome. This structural potential for off-target activity was monitored with internal and external kinase panels, but the lack of kinase activity was maintained throughout the series.

2,4-Dichloropyrimidine underwent selective 4-chloro substitution at room temperature, by reaction with the sodium salt of (S)-4-isopropyl-oxazolidin-2-one (Scheme 1). Subsequent displacement of the 2-chloro at 140 °C with (S)-1-phenylethan-1-amine in DMSO gave (S)-4-isopropyl-3-((S)-1-phenylethylamino)pyrimidin-4-yl)oxazolidin-2-one (**IDH125**, **1f**). The other diastereomers were accessed using the appropriate chiral building blocks.

Scheme 1. Synthetic scheme for **1f** (**IDH125**)



SAR by archive using **IDH125** as the probe structure was unsuccessful in identifying additional molecules in the Novartis compound library with sub-micromolar activity, highlighting that this substructure was somewhat unique. Initial analogs were targeted to explore the tolerance for modification and/or removal of different parts of the molecule (compounds **2a-d**, **3a-f**, and **4a-d** in supporting information). Understanding of this initial SAR was clarified by the determination of the X-ray co-crystal structure of **IDH125** in the homodimer of IDH1^{R132H}, which showed IDH125 binding into an allosteric site adjacent to the substrate binding site.¹³ Replacement of the nitrogen at the 3-position of the pyrimidine with a carbon, and either replacement of the 2-amino with an oxygen or N-alkylation all resulted in loss of activity due to lack of backbone:ligand hydrogen bond donor-acceptor interactions to Leu¹²⁰. Small substituents such as methyl on the 4- and 5-position of the pyrimidine were tolerated. The alpha-methyl of **IDH125** binds into a small nook created by the backbone of Arg¹⁰⁹, Glu¹¹⁰ and Ile¹²⁸ as well as the sidechains of Ile¹³⁰, Ser²⁷⁸ and Met²⁹¹ resulting in a good contact for a methyl group but limited tolerance for larger groups in this region. An unsubstituted oxazolidinone does not lead to the preferred hydrophobic collapse conformation required for binding, but there is tolerance for alternate oxazolidinone substituents beyond isopropyl. Interestingly, the bound structure of **IDH125**¹³ closely overlays with the small molecule X-ray structure, which suggests that hydrophobic collapse drives the molecule to preorder into the active binding conformation. The nature of the residues lining this allosteric pocket are also in stark contrast to those lining the substrate-binding site, and lend a more hydrophobic character to the pocket (Figure 2). This pocket has potential for potent binding of molecules which may also be able to cross the BBB.

Figure 2. Sequence and sidechain representation of the allosteric pocket for IDH1^{R132H}. Amino acids lining the pocket are highlighted in yellow, mutation site R132H is shown in green

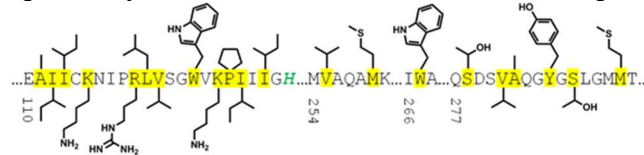
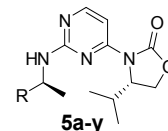
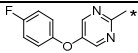
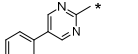
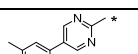


Table 2. IDH1^{R132H} biochemical and HCT116-IDH1^{R132H} cellular activity of analogs exploring phenyl substitution



	R	Biochem LCMS IC ₅₀ / μM	Cellular IC ₅₀ / μM (2-HG)
5a	cyclohexyl	0.35	1.17
5b	2-fluorophenyl	0.19	0.69
5c	3-fluorophenyl	0.25	0.42
5d	4-fluorophenyl	0.15	0.35
5e	3-chlorophenyl	0.18	0.33
5f	4-chlorophenyl	0.13	0.16
5g	3,4-dichlorophenyl	0.097	0.09
5h	2-methoxyphenyl	0.27	0.52

5i	3-methoxyphenyl	0.13	0.43
5k	4-methoxyphenyl	0.3	0.87
5m	3,4-dimethoxyphenyl	0.70	2.5
5n	4-cyanophenyl	0.54	1.34
5p	1-naphthyl	0.25	1.1
5q	2-naphthyl	0.094	0.16
5r	p-biphenyl	0.12	0.17
5s (IDH662)	4-phenoxyphenyl	0.010	0.022
5t	5-chloro pyrimidin-2-yl	2.1	7.9
5v		0.081	0.2
5w[†]		0.34	0.5
5x (IDH889)		0.02	0.014

[†] 1:1 mixture of diastereomers at amine sidechain

The limited ability to improve the potency with simple modifications to the oxazolidinone, alpha-methyl, or pyrimidine regions of **IDH125** necessitated exploration of modifications to the phenyl group (Table 2). Saturation of the phenyl ring and simple substitutions appeared to be tolerated around the ring system (compounds **5a-m**), although larger groups at the *ortho* position were less tolerated than the *meta* or *para* positions. In a similar fashion, 2-naphthyl **5p** is also more potent than 1-naphthyl **5q**. In the *para*-position, the fluoro and chloro groups appeared to give a slight boost in potency, but this was lost with the larger methoxy group. This could have been due to either a steric or electronic effect, but the electron-withdrawing *p*-cyano also showed a drop in potency, suggesting the loss of activity with electron-donating *p*-methoxy was not a wholly electronic effect. Despite the drop in activity for the *p*-methoxy and *p*-cyanophenyl, there was not the precipitous drop usually seen for a steric clash with an inflexible part of the protein. This suggested a low energy sidechain or backbone movement of the protein in this region, which would accommodate larger sidechains (i.e., for these intermediate sized groups the energy penalty for protein reorganization was not being compensated for by the interactions being made in the newly formed pocket). This hypothesis is supported by the potency seen with larger sidechains such as *p*-biphenyl **5r** and *p*-phenoxyphenyl **5s** (**IDH662**). Interestingly, **IDH662** also showed a significant boost in potency vs. the IDH^{wt} protein (IDH^{wt} IC₅₀ 1.03 μM), suggesting that the allosteric pocket is also accessible in the wt protein but is preferentially accessible in the R132 mutated protein.¹³

IDH662 was profiled vs. a panel of *in vitro* assays and showed an overall excellent selectivity for the mutant protein. **IDH662** showed potent cellular inhibition of 2-HG production in the engineered HCT116-IDH1^{R132H} cell line (IC₅₀ 0.022 μM) and inhibition of proliferation in the engineered MCF10A cell-line (IC₅₀ 0.017 μM)¹³ (cell lines available from Horizon Discovery Group plc¹⁵⁻¹⁶). In comparison, **IDH125** was considerably weaker in the HCT-116-IDH1^{R132H} cell line (IC₅₀ 0.66 μM). Despite poor solubility (<5 μM at pH 6.8) and high *in vitro* clearance across species, *in vivo* exposure in mice (AUC 1.1 μM.h, C_{max} 0.39 μM at 10 mg/kg po, AUC 7.9 μM.h, C_{max} 2.5

μM at 100 mg/kg po) was deemed sufficient to explore **IDH662** in an *in vivo* pharmacodynamic (PD) study monitoring compound effects on 2-HG. However, at doses up to 600 mg/kg there was no significant alteration of 2-HG levels in xenograft tumor tissue in the HCT116-IDH1^{R132H} model (data not shown). The estimated free compound concentration from the measured plasma pharmacokinetics (PK) in this study was below the cellular IC₅₀ for mutant IDH1, which suggested that the high plasma protein binding (>99%) limited productive engagement of the target *in vivo*.

It was decided to explore whether *in vivo* modulation of 2-HG inhibition was dependent on free-fraction of drug in the plasma. The high protein binding was likely contributing to a lower *in vivo* clearance than predicted from the *in vitro* microsomal assays, suggesting that lower intrinsic clearance would be needed in tandem with any increase of the free fraction in order to achieve high enough and effective exposures. *In silico* and *in vivo* metabolic studies highlighted the benzylamine as a key source of oxidative metabolic cleavage, so this was the focus of the next iteration of targets.

Heterocyclic replacements of the phenyl group should lower the oxidation potential of the benzylic carbon due to distribution of the local electron density through to the conjugated, and more electronegative, heteroatoms. Heterocycles would also increase the local polarity, and this may be less well tolerated in the binding sites of cytochrome P450 proteins, leading to reduced oxidative metabolism. This is supported by data from Ioannidis *et al*, who have shown excellent *in vitro* and *in vivo* PK properties with a structurally similar halopyrimidine benzylamine for a series of Janus kinase 2 (JAK2) inhibitors.¹⁷

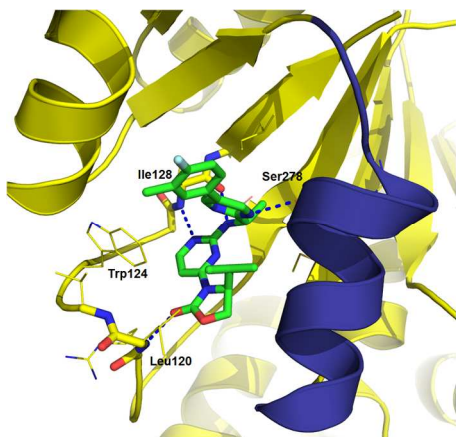
The chemistry used to displace chloro from 2-chloro-4-oxazolidinonyl pyrimidines with benzylamine derivatives was not efficient with less nucleophilic heterocyclic amines such as 1-(5-chloropyrimidin-2-yl)ethylamine. Therefore, the more reactive 2,4-difluoropyrimidine was used to enable the synthesis of the desired products via 2-fluoro-4-oxazolidinonylpyrimidine.

The comparison of chloropyrimidine (**5t**) to chlorophenyl (**5f**) shows a significant improvement in *in vitro* clearance in rat microsomes (CL_{int} 73 μL/min.mg vs. CL_{int} >900 μL/min.mg), but this results in a 16-fold drop in biochemical activity and 50-fold drop in cellular activity. A more moderate 8 to 10-fold drop in activity is observed for the phenoxyphenyl analog **5v** when compared to the analogous phenoxyphenyl **IDH662**. However, <3-fold drop in activity is seen for the phenylpyrimidine analog (diastereomeric mixture **5w** vs. biphenyl **5r**). **5w** also shows an improved clearance in rat microsomes vs. pyrimidine **5t** (**5w** CL_{int} 24 μL/min mg), whereas phenoxy-pyrimidine **5v** was significantly higher (CL_{int} 240 μL/min mg). Pyrimidine and *para*-biaryl motifs were maintained in subsequent analogs, leading to identification of **IDH889** [IDH1^{R132C} IC₅₀ 0.072 μM, IDH1^{WT} IC₅₀ 1.38 μM].

X-ray crystallography of **IDH889** (PDB 5TQH) in homodimer IDH1^{R132H} is consistent with the structure of **IDH125**.¹³ The aminopyrimidine core moiety interacts with the backbone of Ile¹²⁸ via a hydrogen bond donor-acceptor pair, the carbonyl of the oxazolidinone forms a hydrogen bond interaction with Leu¹²⁰, and the alpha-methyl fits into the methyl nook. The molecule is in a hydrophobic collapse conformation with the isopropyl in van-der-Waals contact with the pyrimidine of the amine sidechain. In addition, a hydrogen bond is observed between the pyrimidine of the amine sidechain and Ser²⁷⁸, and this specific interaction may be compensating for the expected

increase in desolvation energy for a more polar ligand (vs. the biphenyl **5r**).

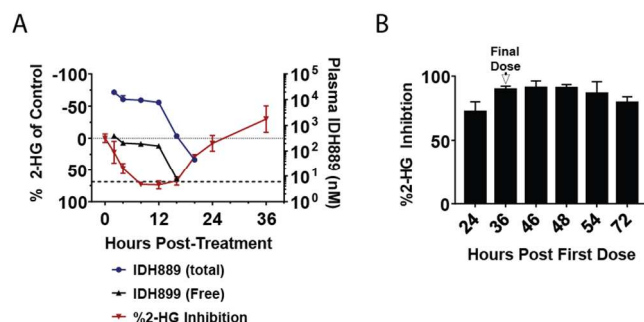
Figure 3. X-ray co-crystal structure of **IDH889** in IDH1^{R132H}.



IDH889 demonstrates significantly improved plasma exposure in mice vs. **IDH662** (AUC 3.6 $\mu\text{M}\cdot\text{h}$, C_{max} 1.7 μM at 10 mg/kg; AUC 55.5 $\mu\text{M}\cdot\text{h}$, C_{max} 14.2 μM at 100 mg/kg). This is coupled with an improved solubility (39 μM at pH 6.8) and measurable free fraction in mouse plasma (98% plasma protein binding), suggesting prolonged plasma concentration 20-fold over the cellular IC_{50} could be achieved at a dose of 100 mg/kg.

In the HCT116-IDH1^{R132H/+} xenograft model, **IDH889** dosed orally at 200 mg/kg inhibits new 2-HG production but does not eliminate 2-HG from IDH1 mutant tissues. Thus, given the high baseline tissue concentration of 2-HG, several hours are required to clear 2-HG from the tissues. Peak reduction in tumor 2-HG levels after a single dose is observed 8-12 hours post administration. 2-HG levels begin to rebound as the free concentration of **IDH889** drops below the *in vitro* cellular IC_{50} (Figure 4A). At 48h post treatment, 2-HG levels return to baseline. Sustained 2-HG inhibition greater than 24 hours was achieved with BID (q12/12) administration of **IDH889** for four doses (Figure 4B).

Figure 4. A) Total and estimated free plasma **IDH889** concentration (mean \pm SD) and percent inhibition of baseline 2-HG levels (mean \pm SEM) in HCT116-IDH1^{R132H} xenograft tumor tissue following a single 200 mg/kg dose (dotted line is zero % inhibition, dashed line represents cellular EC_{50}); B) Percent inhibition (mean \pm SEM) of 2-HG levels in tumor tissue following four doses of **IDH889** at 25mg/kg po bid(q12/12).



In a rat PK study to assess brain:plasma ratio, **IDH889** demonstrates favorable distribution to the brain (30 mg/kg po, 1.4 brain:blood ratio, AUC_{brain} 3117 nM.h, AUC_{blood} 2222 nM.h), albeit with a lower free fraction due to slightly higher rat brain protein binding (99.4%) vs rat plasma protein bind-

ing. **IDH889** also has excellent permeability and no efflux in the Caco-2 and human MDR1-MDCK cell lines, supporting the hypothesis that potent inhibition of mutant IDH1 function by binding at the allosteric binding site is compatible with brain penetration.

It was next tested whether the 2-HG reduction was sufficient to alter DNA methylation, a phenotype closely linked to IDH1 mutation and 2-HG production.¹⁸⁻¹⁹ These studies were performed using Infinium HumanMethylation450 BeadChip arrays (supporting information). Separately derived HCT116-IDH1^{R132H} and HCT116-IDH1^{R132C} cell line clones showed consistent changes in both DNA hyper- and hypomethylation vs. their isogenic wild-type counterpart cell line, that were stable over time (Figure 5A). **IDH889** caused time-dependent changes in these loci, with preferential hypomethylation of the loci in mutant cells that were originally hypermethylated in mutant vs. wild-type cells. Importantly, **IDH889** caused no consistent changes in DNA methylation in the wild-type control cell line, highlighting that the DNA methylation changes in the mutant clones were likely due to IDH1 mutation and 2-HG production. To validate these changes *in vivo*, tumor samples collected at necropsy from the 25 mg/kg bid study (Figure 4B) were evaluated to compare global methylation status vs. tumors obtained from untreated control animals (3 samples/group), as well as parental wildtype (WT) HCT116 tumors. Figure 5B shows that a large number of sites in the genome were either hypermethylated (red,) or hypomethylated (green) in IDH1^{R132H/+} mutant HCT116 tumors vs. WT control tumors. For the sites that were specifically altered in mutant tumors, **IDH889** treatment caused both the hypermethylated and hypomethylated loci to trend towards reversion to their WT status (figure 5C). The sites not altered by R132H mutation (Figure 5B, grey) showed only minor changes as a group upon **IDH889** treatment (data not shown). Together, this data suggests that the level of 2-HG inhibition achieved in Figure 4B was sufficient to modulate mutant IDH1-dependent DNA methylation changes *in vivo*.

In conclusion, a novel HTS hit was optimized for potency and PK properties to generate a tool molecule (**IDH889**) suitable for exploring the effect of inhibition of production of 2-HG by IDH1^{R132H} in preclinical *in vitro* and *in vivo* cancer models. **IDH889** binds into an allosteric, induced-fit pocket in IDH1^{R132H}, has good overall selectivity vs. the WT protein, and inhibits both the IDH1^{R132H} and IDH1^{R132C} mutants, suggesting broad utility across the various known R132* mutations. Oral dosing of **IDH889** in a murine IDH1 mutant tumor xenograft model shows robust reduction of tumor derived 2-HG, a PD biomarker of mutant-IDH1^{R132*} activity. In addition to the potential treatment of AML, chondrosarcoma, cholangiocarcinoma and other forms of mutant-IDH1 driven cancers, **IDH889** demonstrates brain penetrant exposure. This suggests potential utility in preclinical orthotopic tumor models, as well as potential for the series to be optimizable for treating patients with IDH1-mutant brain cancers.

ASSOCIATED CONTENT

Supporting Information

Synthetic procedures, analytical data, assay protocols, SAR of compounds **2a-d**, **3a-f** and **4a-d**, small molecule X-ray data of **IDH125** and **1e**, kinase profiling of **IDH125**, assay protocols, PK and PK/PD study protocols (PDF) is available free of charge on the ACS Publications website.

AUTHOR INFORMATION

Corresponding Authors

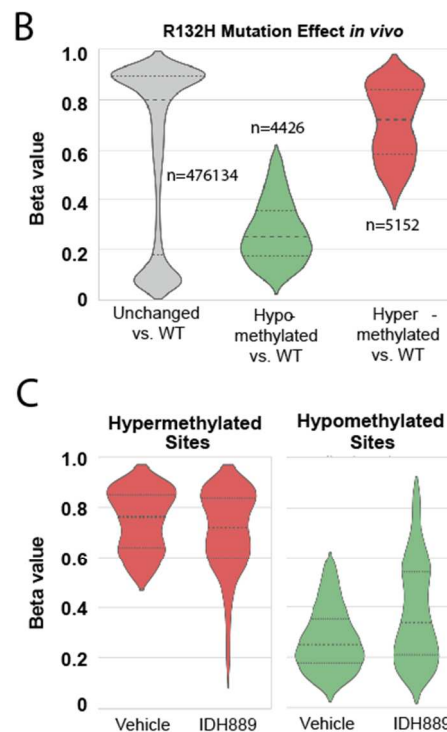
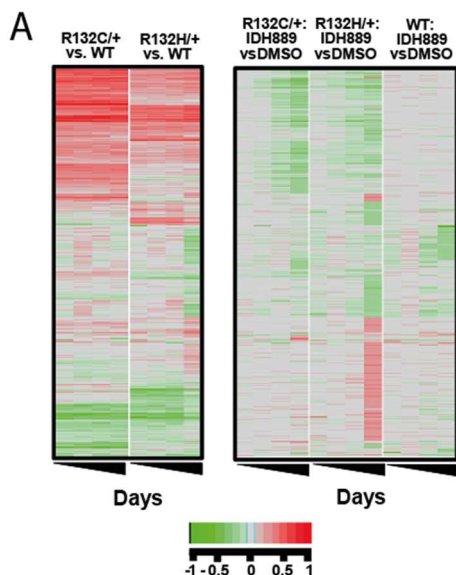
* E-mail: raymond.pagliarini@novartis.com

* E-mail: youngshin.cho@novartis.com

Present Addresses

(J.R.L.) Constellation Pharmaceuticals, 215 First Street, Suite 200, Cambridge, MA 02142; (P.D.F.) and (B.T.) Relay Therapeutics, 215 First Street, Suite 300, Cambridge, MA 02142; (M.X.) Dupont, 1007 Market St. Wilmington, DE 19898; (J.G.) National Cancer Institute, 9609 Medical Center Dr., Rockville, MD 20850; (L.X.Z.) Ipsen Bioscience, Inc., 650 East Kendall Street, Cambridge, MA 02142, USA; (B.F.) Surface Oncology, 215 First Street, Suite 400-S, Cambridge, MA 02142

Figure 5 : A) *In vitro* DNA methylation changes upon **IDH889** treatment in the indicated HCT116 cell clones. Rows represent individual sites in the genome, and columns within each cluster represent time points (days 3, 7, 14, and 28). Green shading indicates hypomethylation and red shading indicates hypermethylation, delta values as described in supporting information. B) Violin plots showing *in vivo* DNA methylation changes in $IDH1^{R132H/+}$ mutant vs. wild-type HCT116 xenograft tumors. Y axis level of methylation for each site (1=methylated, 0=unmethylated: beta values, as described in supporting information), n=number of sites within each group, large dashed line indicates median beta value, and smaller dashed lines indicate 75th (top) and 25th (bottom) percentiles. C) violin plot as in B) for $IDH1^{R132H}$ mutant tumors after treatment with **IDH889** (tumors from Figure 4B).



ACKNOWLEDGMENT

The authors would like to thank Thomas Smith, Kimberley Yue, and Daniel Baird for screen optimization and execution; Kara Herlihy, Tami Hood, and Suzanne Zhu for their help with the development of the in-vitro activity assays; and Bill Sellers, Markus Warmuth, Karin Briner, Juerg Zimmerman, Tim Ramsey and Travis Stams for project support.

REFERENCES

- (1) Cairns, R.A.; Mak, T.W.; Oncogenic isocitrate dehydrogenase mutations: mechanisms, models, and clinical opportunities. *Cancer Discovery* **2013**, *3*, 730-41.
- (2) Dang, L.; White, D.W.; Gross, S.; Bennett, B.D.; Bittinger, M.A.; Driggers, E.M.; Fantin, V.R.; Jang, H.G.; Jin, S.; Keenan, M.C.; Marks, K.M.; Prins, R.M.; Ward, P.S.; Yen, K.E.; Liau, L.M.; Rabinowitz, J.D.; Cantley, L.C.; Thompson, C.B.; Vander Heiden, M.G.; Su, S.M.; Cancer-associated IDH1 mutations produce 2-hydroxyglutarate. *Nature* **2009**, *462*, 739-44.
- (3) Losman, J.A.; Kaelin, W.G., Jr.; What a difference a hydroxyl makes: mutant IDH, (R)-2-hydroxyglutarate, and cancer. *Genes Dev.* **2013**, *27*, 836-52.
- (4) Popovici-Muller, J.; Saunders, J. O.; Salituro, F.G.; Travins, J.M.; Yan, S.; Zhao, F.; Gross, S.; Dang, L.; Yen, K.E.; Yang, H.; Straley, K.S.; Jin, S.; Kunii, K.; Fantin, V.R.; Zhang, S.; Pan, O.; Shi, D.; Biller, S.A.; Su, S.M.; Discovery of the first potent inhibitors of mutant IDH1 that lower tumor 2-HG in vivo. *ACS Med. Chem. Lett.* **2012**, *3*, 850-5.
- (5) Brooks, E.; Wu, X.; Hanel, A.; Nguyen, S.; Wang, J.; Zhang, J.; Harrison, A.; Zhang, W.; Identification and characterization of small-molecule inhibitors of the R132H/R132H mutant isocitrate dehydrogenase 1 homodimer and R132H/wild-type heterodimer. *J. Biomol. Screen.* **2014**, *19*, 1193-1200.
- (6) Deng, G.; Shen, J.; Yin, M.; McManus, J.; Mathieu, M.; Gee, P.; He, T.; Shi, C.; Bedel, O.; McLean, L.R.; Le-Strat, F.; Zhang, Y.; Marquette, J.P.; Gao, Q.; Zhang, B.; Rak, A.; Hoffmann, D.; Rooney, E.; Vassort, A.; Englaro, W.; Li, Y.; Patel, V.; Adrian, F.; Gross, S.; Wiederschain, D.; Cheng, H.; Licht, S.; Selective inhibition of mutant isocitrate dehydrogenase 1 (IDH1) via disruption of a metal binding

network by an allosteric small molecule. *J. Biol. Chem.* **2015**, *290*, 762-74.

(7) Okoye-Okafor, U.C.; Bartholdy, B.; Cartier, J.; Gao, E.N.; Pietrak, B.; Rendina, A.R.; Rominger, C.; Quinn, C.; Smallwood, A.; Wiggall, K.J.; Reif, A.J.; Schmidt, S.J.; Qi, H.; Zhao, H.; Joberty, G.; Faelth-Savitski, M.; Bantscheff, M.; Drewes, G.; Duraiswami, C.; Brady, P.; Groy, A.; Narayanagari, S.R.; Antony-Debre, I.; Mitchell, K.; Wang, H.R.; Kao, Y.R.; Christopheit, M.; Carvajal, L.; Barretero, L.; Paietta, E.; Makishima, H.; Will, B.; Concha, N.; Adams, N.D.; Schwartz, B.; McCabe, M.T.; Maciejewski, J.; Verma, A.; Steidl U.; New IDH1 mutant inhibitors for treatment of acute myeloid leukemia. *Nat. Chem. Biol.* **2015**, *11*, 878-86.

(8) Rohle, D.; Popovici-Muller, J.; Palaskas, N.; Turcan, S.; Grommes, C.; Campos, C.; Tsoi, J.; Clark, O.; Oldrini, B.; Komisopoulou, E.; Kunii, K.; Pedraza, A.; Schalm, S.; Silverman, L.; Miller, A.; Wang, F.; Yang, H.; Chen, Y.; Kernysky, A.; Rosenblum, M.K.; Liu, W.; Biller, S.A.; Su, S.M.; Brennan, C.W.; Chan, T.A.; Graeber, T.G.; Yen, K.E.; Mellinghoff, I.K.; An inhibitor of mutant IDH1 delays growth and promotes differentiation of glioma cells *Science* **2013**; *340* (6132), 626-630.

(9) Zheng, B.; Yao, Y.; Liu, Z.; Deng, L.; Anglin, J.L.; Jiang, H.; Prasad, B.V.V.; Song Y.; Crystallographic investigation and selective inhibition of mutant isocitrate dehydrogenase. *ACS Med. Chem. Lett.* **2013**, *4*, 542.

(10) Liu, Z.; Yao, Y.; Kogiso, M.; Zheng, B.; Deng, L.; Qiu, J.J.; Dong, S.; Lv, H.; Gallo, J.M.; Li, X.-N.; Song, Y.; Inhibition of cancer-associated mutant isocitrate dehydrogenases: synthesis, structure-activity relationship, and selective antitumor activity *J. Med. Chem.* **2014**, *57*, 8307-8318.

(11) Fan, B.; Le, K.; Manyak, E.; Liu, H.; Prah, M.; Bowden, C. J.; Biller, S.; Agresta, S.; Yang, H.; Longitudinal pharmacokinetic/pharmacodynamic profile of AG-120, a potent inhibitor of the IDH1 mutant protein, in a phase 1 study of IDH1-mutant advanced hematologic malignancies *Blood*, **2015**, *126*, 1310.

(12) Rankovic, Z. CNS Drug Design: Balancing physicochemical properties for optimal brain exposure, *J. Med. Chem.* **2015**, *58*, 2584.

(13) Xie, X.; Capka, V.; Chen, J.; Chenail, G.; Cho, Y.S.; Dooley, J.; Farsidjani, A.; Fortin, P.D.; Kohl, D.; Kulathila, R.; Lin, F.; McKay, D.; Sage, D.; van der Plas, S.; Wright, K.; Xu, M.; Yin, H.; Levell, J.; Pagliarini, R.A.; Allosteric mutant IDH1 inhibitors reveal mechanisms for IDH1 mutant and isoform selectivity *Structure* **2016** (submitted).

(14) Wu, P.; Nielsen, T.E.; Clausen, M.H.; Small-molecule kinase inhibitors: an analysis of FDA-approved drugs, *Drug Discovery Today* **2016**, *21*(1), 5.

(15) Horizon Discovery Group plc, 7100 Cambridge Research Park, Waterbeach, Cambridge, CB25 9TL, United Kingdom. www.horizondiscovery.com Human IDH1(R132H/+) HCT116 cell line : HD 104-013; Human IDH1(R132H/+) MCF10A cell line : HD 101-013.

(16) <http://www.ncbi.nlm.nih.gov/pubmed/23038259>.

(17) Ioannidis, S.; Lamb, M.L.; Wang, T.; Almeida, L.; Block, M.H.; Davies, A.M.; Peng, B.; Su, M.; Zhang, H.-J.; Hoffmann, E.; Rivard, C.; Green, I.; Howard, T.; Pollard, H.; Read, J.; Alimzhanov, M.; Beberitz, G.; Bell, K.; Ye, M.; Huszar, D.; Zinda, M.; Discovery of 5-chloro-N²-[(1S)-1-(5-fluoropyrimidin-2-yl)ethyl]-N⁴-(5-methyl-1H-pyrazol-3-yl)-pyrimidine-2,4-diamine (AZD1480) as a novel inhibitor of the JAK/STAT pathway, *J. Med. Chem.* **2011**, *54*, 262.

(18) Turcan, S.; Rohle, D.; Goenka, A.; Walsh, L.A.; Fang, F.; Yilmaz, E.; Campos, C.; Fabius, A. W.; Lu, C.; Ward, P. S.; Thompson, C. B.; Kaufman, A.; Guryanova, O.; Levine, R.; Heguy, A.; Viale, A.; Morris, L. G.; Huse, J. T.; Mellinghoff, I. K.; Chan, T. A.; IDH1 mutation is sufficient to establish the glioma hypermethylator phenotype. *Nature* **2012**, *483*, 479.

(19) Duncan, C. G.; Barwick, B. G.; Jin, G.; Rago, C.; Kapoor-Vazirani, P.; Powell, D. R.; Chi, J. T.; Bigner, D. D.; Vertino, P. M.; Yan, H.; A heterozygous IDH1R132H/WT mutation induces genome-wide alterations in DNA methylation *Genome Res.* **2012**, *22*, 2339.

For Table of Contents Use Only

Optimization of 3-Pyrimidin-4-yl-oxazolidin-2-ones as Allosteric and Mutant Specific Inhibitors of IDH1

Julian R. Levell, Thomas Caferro, Gregg Chenail, Ina Dix, Julia Dooley, Brant Firestone, Pascal D. Fortin, John Giraldes, Ty Gould, Joseph D. Growney, Michael D. Jones, Raviraj Kulathila, Fallon Lin, Gang Liu, Arne Mueller, Simon van der Plas, Kelly Slocum, Troy Smith, Remi Terranova, B. Barry Touré, Viraj Tyagi, Trixie Wagner, Xiaoling Xie, Ming Xu, Fan S. Yang, Liping X. Zhou, Raymond Pagliarini,* and Young Shin Cho*

Novartis Institutes for Biomedical Research, 250 Massachusetts Avenue, Cambridge, MA 02139

Graphical Abstract:

